Fasting 2-Deoxy-2-[^{18}F]fluoro-D-glucose Positron Emission Tomography to Detect Metabolic Changes in Pulmonary Arterial Hypertension Hearts over 1 Year

Erika L. Lundgrin[1], Margaret M. Park[2], Jacqueline Sharp[3], W.H. Wilson Tang[2], James D. Thomas[2], Kewal Asosingh[3], Suzy A. Comhair[3], Frank P. DiFilippo[4], Donald R. Neumann[4], Laura Davis[5], Brian B. Graham[5], Rubin M. Tuder[5], Iva Dostanic[1], and Serpil C. Erzurum[3,6]

[1]Cleveland Clinic Lerner College of Medicine, Cleveland, Ohio; [2]Heart & Vascular Institute [4]Department of Nuclear Medicine, and [6]Respiratory Institute, Cleveland Clinic, Cleveland, Ohio; [3]Department of Pathobiology, Lerner Research Institute, Cleveland, Ohio; and [5]Program in Translational Lung Research, University of Colorado School of Medicine, Aurora, Colorado

Abstract

Background: The development of tools to monitor the right ventricle in pulmonary arterial hypertension (PAH) is of clinical importance. PAH is associated with pathologic expression of the transcription factor hypoxia-inducible factor (HIF)-1α, which induces glycolytic metabolism and mobilization of proangiogenic progenitor ($CD34^+CD133^+$) cells. We hypothesized that PAH cardiac myocytes have a HIF-related switch to glycolytic metabolism that can be detected with fasting 2-deoxy-2-[^{18}F]fluoro-D-glucose positron emission tomography (FDG-PET) and that glucose uptake is informative for cardiac function.

Methods: Six healthy control subjects and 14 patients with PAH underwent fasting FDG-PET and echocardiogram. Blood $CD34^+CD133^+$ cells and erythropoietin were measured as indicators of HIF activation. Twelve subjects in the PAH cohort underwent repeat studies 1 year later to determine if changes in FDG uptake were related to changes in echocardiographic parameters or to measures of HIF activation.

Measurements and Results: FDG uptake in the right ventricle was higher in patients with PAH than in healthy control subjects and correlated with echocardiographic measures of cardiac dysfunction and circulating $CD34^+CD133^+$ cells but not erythropoietin. Among patients with PAH, FDG uptake was lower in those receiving β-adrenergic receptor blockers. Changes in FDG uptake over time were related to changes in echocardiographic parameters and $CD34^+CD133^+$ cell numbers. Immunohistochemistry of explanted PAH hearts of patients undergoing transplantation revealed that HIF-1α was present in myocyte nuclei but was weakly detectable in control hearts.

Conclusions: PAH hearts have pathologic glycolytic metabolism that is quantitatively related to cardiac dysfunction over time, suggesting that metabolic imaging may be useful in therapeutic monitoring of patients.

Keywords: hypoxia-inducible factor 1, alpha subunit; positron emission tomography; fluorodeoxyglucose F18; right ventricle; heart failure

(Received in original form June 15, 2012; accepted in final form August 18, 2012)

Support: National Heart, Lung and Blood Institute grant HL60917 and National Institutes of Health grant T35 HL082544.

Correspondence and requests for reprints: Serpil C. Erzurum, M.D., 9500 Euclid Avenue/NC22, Cleveland, OH 44195.
E-mail: erzurus@ccf.org

Ann Am Thorac Soc Vol 10, No 1, pp 1–9, Feb 2013

DOI: 10.1513/AnnalsATS.201206-029OC
Internet address: www.atsjournals.org

Introduction

Despite recent advancements in the diagnosis, management, and treatment of pulmonary arterial hypertension (PAH), this disease of increased pulmonary vascular resistance remains a progressive illness with significant morbidity and mortality secondary to progressive right ventricular failure (1–4). The development of tools to monitor the response of the right ventricle (RV) in this disease is therefore of clinical value. Although the healthy heart derives the majority of its energy from free fatty acid metabolism (5), the PAH heart has been shown to undergo a switch to glycolytic metabolism (6–8), but the mechanism by which metabolic changes occur in PAH remains poorly understood. The proliferative angiopathy in PAH lungs has been mechanistically linked to pathologic expression of hypoxia-inducible factor (HIF)-1α, the regulatory subunit of the HIF transcription factor that increases the

expression of genes involved in glycolysis, angiogenesis, and erythropoiesis (9). HIF-1α promotes the expression of genes that lead to proliferation and mobilization of proangiogenic progenitors ($CD34^+CD133^+$ cells) from the bone marrow, which fuel pulmonary vascular remodeling (10). HIF activation has also been linked to a shift to glycolytic metabolism in pulmonary hypertensive endothelial cells (11, 12). *In vivo* positron emission tomography (PET) imaging of patients with PAH reveals increased uptake of the glucose analog tracer 2-deoxy-2-[^{18}F]fluoro-D-glucose (FDG) in PAH lungs. Here, we hypothesized that cardiac myocytes in PAH also switch to glycolytic metabolism due to HIF-1 activation and that this metabolic switch relates to myocardial and clinical parameters of disease severity. To investigate this, we measured fasting FDG uptake in the hearts of patients with PAH in comparison to healthy control subjects and after 1 year of follow-up, in relation to echocardiographic and clinical parameters of disease, and evaluated whether glycolytic metabolism was associated with HIF-activated effectors. Some of the results of this study have been previously reported in the form of an abstract (13).

Methods

Study Design and Population

Healthy control subjects and patients diagnosed with idiopathic, hereditary, or associated PAH according to the revised clinical classification of pulmonary hypertension (Dana Point 2008) between the ages of 18 and 65 years were recruited for the study. Those with cancer, diabetes mellitus, chronic hemolytic anemia, or arterial hypoxemia were not eligible to participate. Enrolled participants underwent an FDG-PET scan, echocardiography, and a blood draw at baseline; patients with PAH additionally underwent the 6-minute-walk test and clinical status assessment and returned for repeat studies 1 year later. All subjects provided informed consent to participate in the study, which was approved by the Cleveland Clinic Institutional Review Board.

FDG-PET Scan

Subjects fasting at least 6 hours were injected with 370 MBq (10 mCi) of the glucose tracer FDG and imaged sequentially using a hybrid PET/CT system 1.5 hours after injection. Finger stick blood glucose level was measured before the scan to assure blood glucose was than 120 mg/dl. Images were analyzed by a single blinded radiologist using an image fusion workstation (Syngo TrueD; Siemens Molecular Imaging, Hoffman Estates, IL) with region-of-interest–measuring tools. The average standardized uptake value (SUV) of FDG was measured in the RV, right atrium (RA), interventricular septum (IVS), left ventricle (LV), and the blood pool of the thoracic aorta. FDG uptake in each heart region was then normalized for the amount of FDG measured in the blood pool, calculated as follows:

(average FDG-SUV in region of interest)/(average FDG-SUV in blood pool of thoracic aorta).

Echocardiography

Doppler echocardiography was performed by a single experienced echocardiographer to evaluate right ventricular structure and function using principles outlined in the guidelines from the American Society of Echocardiography (14). RV end-diastolic and end-systolic areas were measured in the apical four-chamber view by tracing the endocardial border of the RV and the tricuspid annular plane. RV fractional area change was calculated as follows:

[(RV end-diastolic area minus RV end-systolic area)/RV end-diastolic area]×100.

Right atrial volume was measured in the apical four-chamber view by using the single-plane area-length method. The peak pulmonary artery systolic pressure (PASP) was estimated from the systolic pressure gradient between the RV and the right atrium by the peak continuous-wave Doppler velocity of the tricuspid regurgitant jet using the modified Bernoulli equation plus estimated right atrial pressure (RAP). RAP was estimated from the subcostal window approach measuring changes in inferior vena caval size and collapsibility as determined by the respiratory sniff test following American Society of Echocardiography guidelines. The systolic and diastolic eccentricity index was calculated as the ratio of the LV anteroposterior diameter divided by the LV septal-lateral diameter. This serves as an indirect measure of RV pressure and volume overload (15, 16). RV global longitudinal strain was measured using two-dimensional speckle-tracking echocardiography. Briefly, the technology allows tracking of small, temporally stable, and unique myocardial features, referred to as speckles, using block-matching to provide local displacement information from which parameters of myocardial function, such as velocity and strain, can be derived. Strain refers to a fractional change in length of a myocardial segment, with shortening in length expressed as a negative value by convention. RV global longitudinal strain is the average of the strain of all the RV myocardial segments evaluated.

Clinical Status Assessment

WHO/NYHA functional status was classified for each patient (I–IV) based on symptom severity (17). Standard clinical labs were collected at each visit, including complete blood count, metabolic panel, and B-type natriuretic peptide test. To assess functional capacity, patients underwent the 6-minute-walk test at each visit, performed according to American Thoracic Society (ATS) guidelines (18). Briefly, the distance that each patient with PAH could walk as quickly as possible on a flat, hard surface in 6 minutes was measured in feet. To determine whether the patients remained clinically stable over time, a blinded pulmonologist and cardiologist reviewed each patient's echocardiographic, 6-minute-walk, and B-type natriuretic peptide data to independently classify each patient as clinically improving, worsening, or remaining stable over the year. Clinical worsening was defined as having at least two of the following: (*1*) increase in WHO functional class, (*2*) increase in estimated RAP of 5 mm Hg or more, and (*3*) increase in RV end diastolic area by at least 10% (19). Any status discrepancies between the two clinicians were reviewed by a third blinded pulmonologist to determine final clinical status classification.

Biomarkers of HIF Activation

Ethylenediaminetetraacetic acid blood samples were collected from patients with PAH for measurement of circulating $CD34^+CD133^+$ cells via flow cytometry as described previously (20) and of plasma erythropoietin by ELISA (R&D Systems, Minneapolis, MN).

Immunohistochemistry

HIF-1α expression was evaluated by immunohistochemistry of formalin-fixed paraffin–embedded tissue from explanted PAH hearts of separate patients undergoing transplantation in comparison to donor hearts not used in transplantation with no known cardiac pathology. Antigen retrieval was done by boiling the sections in citrate buffer (Vector #H3300) for 50 minutes followed by treatment with 3% H_2O_2 twice, 5 minutes each time, and avidin and biotin blocks for 10 minutes each. The Dako Catalyzed Signal Amplification (CSA) protein block (Dako #K1500) was performed for 15 minutes followed by incubation with the primary mouse monoclonal HIF-1α antibody (Novus Biological NB 100–123) at 1:8,000 dilution for 30 minutes. The link antibody, streptavidin-biotin complex, amplification reagent, and streptavidin-HRP from the CSA kit were then used according to the manufacturer's protocol. The sections were developed using diaminobenzidine as the chromagen, and no counterstain was used.

Statistical Analysis

Data are reported in aggregate as mean ± SEM or median (range) for continuous data and as n (%) for categorical data. Statistical comparisons were performed using ANOVA or nonparametric equivalent as appropriate. Changes in the PAH cohort over time are reported as the percent change from baseline divided by follow-up time in years and were analyzed by paired *t* test or nonparametric equivalent as needed. Spearman correlation coefficients were used to detect associations between fasting FDG-PET, laboratory, and clinical parameters. Significance was set at an α of 0.05. Data were analyzed using the JMP 9 statistical software (SAS Institute, Cary, NC).

Results

Clinical Characteristics

Six healthy control subjects and 14 patients with PAH consented to participate in the study; 12 patients with PAH were available for repeat studies at 1.04 ± 0.04 years of follow-up. Patients PAH were predominantly WHO functional class II and classified as idiopathic. Patients and healthy control subjects were similar in terms of baseline demographics, and the PAH cohort remained relatively stable in terms of clinical status over the year of follow-up (Table 1). Patient medications at baseline included sildenafil (n = 7), bosentan (n = 6), ambrisentan (n = 2), epoprostenol (n = 5), treprostinil (n = 6), digoxin (n = 6), warfarin (n = 8), β blockers (n = 5), calcium channel blockers (n = 3), and diuretics (n = 9). All patients were being treated with at least one PAH-specific therapy (endothelin

Table 1. Clinical characteristics of study participants at baseline and 1 year*

Characteristic	Control (*n = 6*)	PAH Baseline (*n = 14*)	PAH at 1 yr (*n = 12*)
PAH subgroup (idiopathic/ hereditary/associated)	—	9/3/2	8/2/1
WHO functional class (I/II/III/IV)	—	1/12/1/0	1/10/0/1
Age, yr	44 ± 3	46 ± 3	45 ± 3
Race, caucasian/African American	6/0	13/1	11/1
Sex, M/F	0/6	3/11	3/9
Heart rate, beats/min	65 ± 6	74 ± 3	75 ± 4
BMI, kg/m^2	30 ± 4	27 ± 1	27 ± 1
MAP, mm Hg	91 ± 6	77 ± 3	80 ± 2
6-min-walk distance, ft	—	1,580 ± 92	1,579 ± 96
Sp_{O_2} during walk, %†	—	93 ± 1	94 ± 1
BNP, pg/ml‡	—	124 ± 56	122 ± 41

Definition of abbreviations: BMI = body mass index; BNP = B-type natriuretic peptide; MAP = mean arterial pressure; PAH = pulmonary arterial hypertension; WHO = World Health Organization.
*Data presented as mean ± SEM or as n. Paired *t* tests revealed no significant changes over 1 yr ($P > 0.3$, except age, where $P < 0.0001$). There were no significant differences between control and participants with PAH,at baseline ($P > 0.05$).
†On room air except one patient on a 2-liter nasal cannula at baseline.
‡Only available for 12 patients at baseline and 10 patients at follow-up.

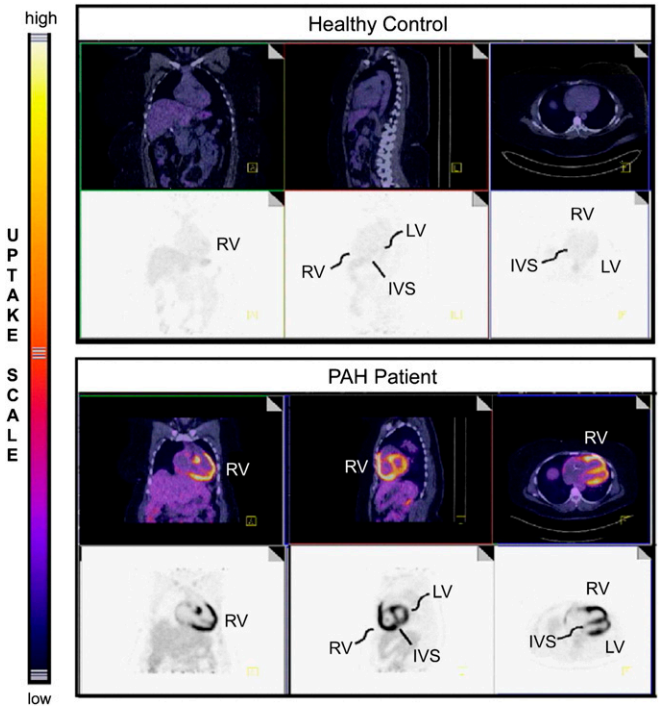

Figure 1. Fasting 2-deoxy-2-[^{18}F]fluoro-D-glucose positron emission tomography (FDG-PET) imaging of control participant and patient with pulmonary arterial hypertension (PAH). Fasting FDG-PET imaging reveals generalized enhanced FDG standardized uptake value in the PAH heart. IVS = interventricular septum; LV = left ventricle; RV = right ventricle.

antagonist, phosphodiesterase-5 inhibitor, and prostanoid) throughout the study period, with six patients on two agents and three patients on three agents at baseline. Only one patient in the cohort was started on a new PAH-specific therapy (sildenafil added to treprostinil) between the two study visits. Two patients were unavailable at the 1-year follow-up visit; one underwent lung transplantation, and the other was lost to follow-up.

Glucose Uptake Was Increased in PAH Hearts *In Vivo*

Although patients with PAH tended to have increased fasting FDG uptake globally throughout the heart compared with relatively little uptake in healthy subjects (Figure 1), relative FDG-SUV was only significantly higher in the right heart regions (RV and RA) of patients with PAH compared with the hearts of healthy control subjects at baseline (Figure 2) (LV: PAH 4.3 [1.2–17.4], control subjects 2.6 [0.4–10.1], $P = 0.34$; IVS: PAH 4.0 [1.4–17.7], control subjects 1.9 [1.0–7.3], $P = 0.08$; RV: PAH 4.4 [1.0–12.7], control subjects 1.0 [0.8–6.8], $P = 0.02$; RA: PAH 1.3 [0.7–3.3], control subjects 0.8 [0.4–1.0], $P = 0.04$). There was no significant difference in blood pool FDG-SUV. Mean blood glucose by finger stick of patients undergoing fasting FDG-PET was 91 $\pm$ 2 mg/dl at baseline (one value missing but criteria of < 120 were met) and 88 $\pm$ 2 mg/dl at 1-year follow-up, supporting that images were acquired under fasting conditions.

Right Heart FDG-SUV Is Relatively Stable Over Time

As assessed by blinded clinicians, only two patients appeared to clinically worsen over the year (one with idiopathic and one with hereditary PAH), whereas three clinically improved over the year (two with IPAH and one with associated PAH); the remaining seven patients were considered clinically unchanged (five IPAH, one HPAH, and one APAH). In this cohort of patients with clinically stable PAH, FDG-SUV of the right heart also remained relatively stable over 1 year, whereas LV and IVS FDG-SUV tended to decrease over the year (Figure 3).

Indicators of HIF Activation Are Related to Fasting FDG Uptake

Previous studies have identified greater mobilization of bone marrow progenitors and higher levels of erythropoietin in patients with PAH as compared with healthy control subjects (10, 20). Here, we evaluated whether levels of circulating bone marrow progenitor $CD34^+CD133^+$ cells or plasma erythropoietin were correlated to fasting relative FDG-SUV of PAH hearts. Circulating $CD34^+CD133^+$ cells in patients with PAH were positively related to fasting FDG uptake in the RA and RV at baseline (Figure 4A). However, percent circulating $CD34^+CD133^+$ cells tended to decrease over time (paired data available for eight subjects: baseline 0.108 $\pm$ 0.017, 1 yr 0.076 $\pm$ 0.012, paired t test, $P = 0.086$), and the percent change in circulating proangiogenic precursors was negatively correlated with the percent change in FDG-SUV of both ventricles (Figure 4B). In contrast, plasma

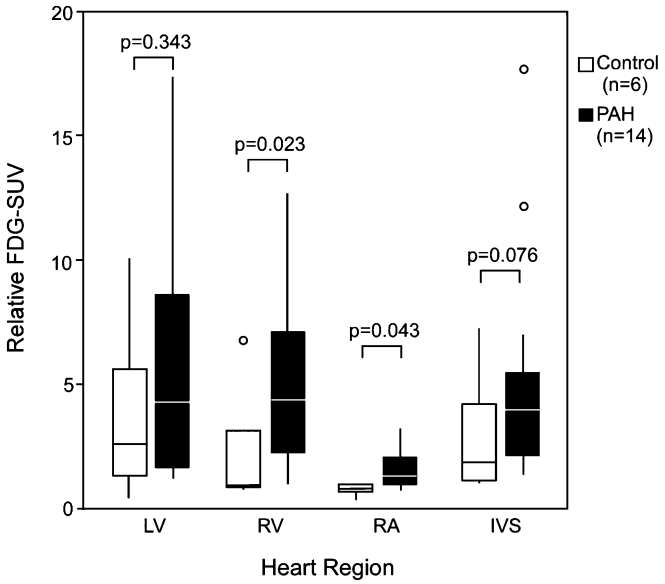

Figure 2. Baseline fasting relative 2-deoxy-2-[^{18}F]fluoro-D-glucose standardized uptake value (FDG-SUV) in pulmonary arterial hypertension (PAH) and control hearts. Box plot representation of the relative FDG-SUV at baseline in four heart regions: right atrium (RA), right ventricle (RV), left ventricle (LV), and interventricular septum (IVS). *P* values reported are from the two-sided rank-sums test. Fasting relative FDG-SUV is increased in PAH RV and RA compared with control subjects.

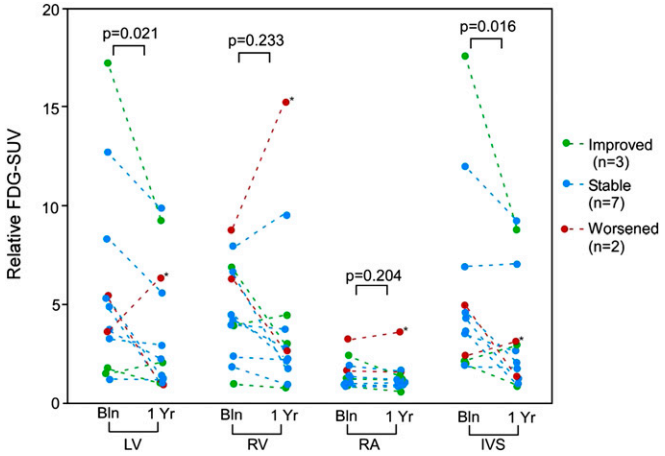

Figure 3. Changes in fasting relative 2-deoxy-2-[^{18}F]fluoro-D-glucose standardized uptake value (FDG-SUV) over 1 year by clinical status classification. Fasting relative FDG-SUV of patients with pulmonary arterial hypertension (PAH) is shown at baseline and at 1 year in four heart regions: (right atrium [RA], right ventricle [RV], left ventricle [LV], and interventricular septum [IVS]), by clinical status classification (improved, stable, or worsened). *P* values reported are from the signed rank test. Each *dashed line* represents an independent PAH patient. *WHO functional class III-IV patient who was transplanted a month after the 1-year visit.

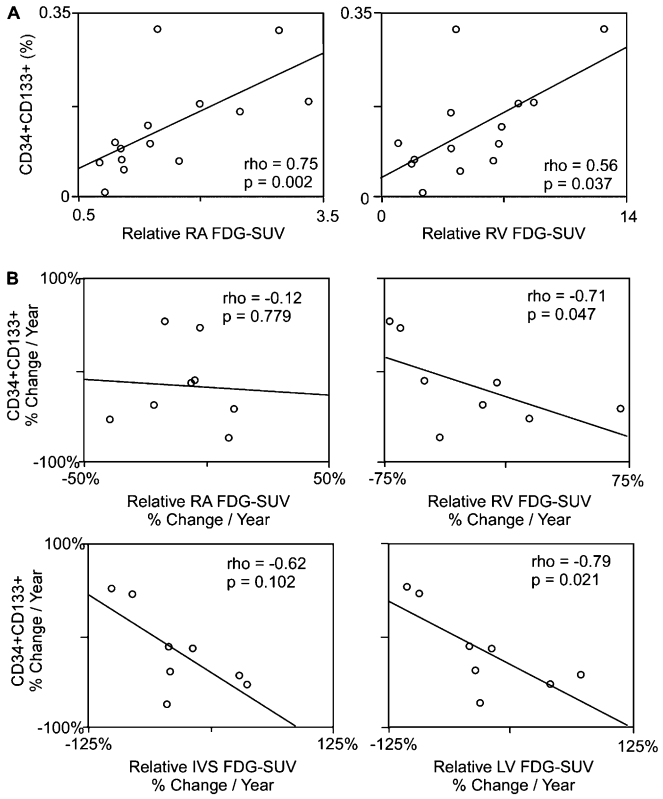

Figure 4. Fasting relative 2-deoxy-2-[^{18}F]fluoro-D-glucose standardized uptake value (FDG-SUV) relates to circulating $CD34^+CD133^+$ cells in pulmonary arterial hypertension (PAH). Each *open circle* represents an independent patient with PAH. At baseline, there is a positive relationship between right atrium (RA) and right ventricle (RV) FDG-SUV and % circulating $CD34^+CD133^+$ cells. However, percent change in circulating progenitors over 1 year negatively correlates to percent change in relative FDG-SUV of the RV and LV. IVS = interventricular septum.

erythropoietin was not related to relative FDG uptake of the RV or RA (data not shown). In a separate small cohort of deidentified heart tissue samples, HIF-1α expression was directly evaluated in hearts explanted from patients with PAH undergoing lung transplantation (n = 2) and donor control hearts not used in transplantation (n = 3). HIF-1α immunoreactivity was present in PAH nuclei of myocytes but was weak or not detectable in control hearts (Figure 5). The relationship of circulating $CD34^+CD133^+$ cells to glucose uptake of the right heart and the presence of HIF-1α in hearts of patients with PAH suggests that the switch to glycolytic metabolism may be HIF related.

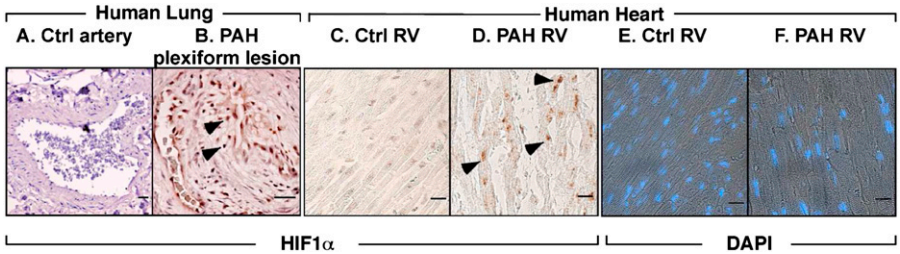

Figure 5. Hypoxia-inducible factor (HIF)-1α protein expression in pulmonary arterial hypertension (PAH) plexiform lesions and cardiac myocytes. *Arrows* point to a few of the many brown-staining nuclei of PAH pulmonary endothelial cells (*B*) and cardiac myocytes (*D*). Nuclear localization was confirmed by sequential sections of heart in which nuclei were identified by DAPI (*blue*) immunofluorescence (*E*, *F*). Scale bar: 25 μm. Ctrl = control; RV = right ventricle.

Right Heart Fasting FDG Uptake Relates to Echocardiographic Indices of Heart Failure

Although no relationship between estimated RV systolic pressure and RV FDG-SUV was detected in this cohort, fasting relative FDG uptake in the right side of the heart was associated with other echocardiographic markers of right ventricular structure and function. In patients with PAH, right heart FDG uptake was strongly and significantly positively related to RV end systolic diameter, systolic eccentricity index, and RV global strain and was strongly negatively related to RV fractional area change and RV outflow tract velocity–time integral (Figure 6). Over 1 year, percent changes in right heart FDG-SUV correlated with changes in echocardiographic disease severity measures; RA FDG-SUV changes related to changes in RA pressure and RV systolic pressure, whereas RV FDG-SUV changes related to changes in PR grade and LV end diastolic length (Figure 7).

Discussion

This study identifies that fasting relative FDG-SUV of the PAH heart is quantitatively related to echocardiographic markers of disease severity, suggesting that fasting FDG-PET is an indicator of right heart metabolic and structural dysfunction. These metabolic changes in the heart may be due to HIF activation, although this could not be directly measured in this study. Although prior studies have evaluated FDG-SUV in the heart in patients with pulmonary hypertension (6–8, 21–24), to our knowledge we are the first to report longitudinal FDG-PET data in PAH. Additionally, most prior studies used a glucose bolus before FDG infusion, which induces the release of endogenous insulin to enhance glucose uptake by all tissues; under these conditions, healthy myocardium robustly takes up FDG (7, 21–24). In contrast, in the current study, the glucose analog tracer was infused under fasting conditions, under which normal myocardial FDG uptake is low to undetectable. The increased fasting FDG uptake by PAH hearts suggests a switch from predominantly fatty acid to glucose metabolism, as has been described in the pulmonary vasculature of patients with PAH (11) and established in animal models of the disease (25). There was no overall significant change in FDG uptake over 1 year in patients who were clinically stable.

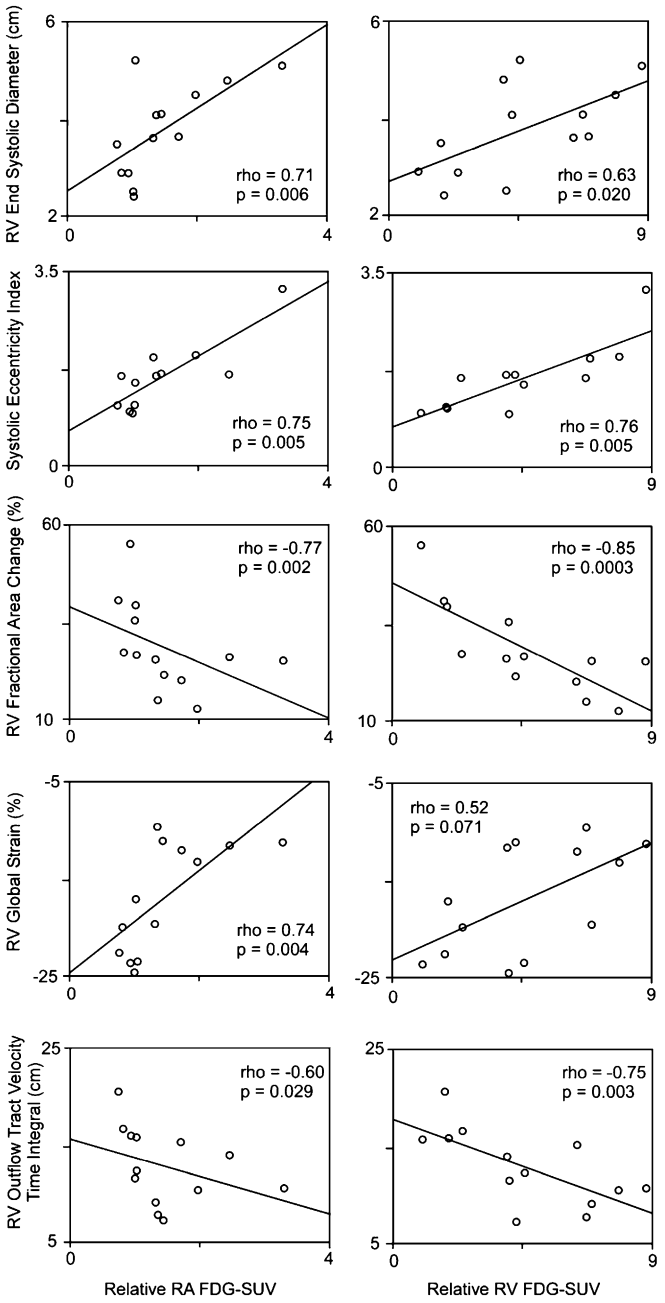

Figure 6. Relative 2-deoxy-2-[^{18}F]fluoro-D-glucose (FDG) uptake of right ventricle (RV) and right atrium (RA) relates to echocardiographic parameters in pulmonary arterial hypertension (PAH). Each *open circle* represents an independent patient with PAH at the baseline visit.

Two cross-sectional studies using fasting FDG-PET imaging have also revealed a greater RV FDG-SUV in patients with PAH as compared with control subjects (6, 8). In one study, the RV/LV FDG uptake ratio correlated to echocardiographic parameters of RV function, including the RV Tei index and the ratio of the RV to LV diastolic areas (6). As in our study, RV FDG-SUV did not correlate with severity of estimated PASP. This dissociation between estimated PASP and fasting FDG uptake in both the prior and current study is consistent with the finding that pulmonary artery pressure relates poorly to RV function or survival (26, 27).

Independent of the relationship between RV metabolism, structure, and function, the current study also links the glycolytic shift of the PAH RV to the percent of circulating $CD34^+CD133^+$ cells. Mobilization of $CD34^+CD133^+$ proangiogenic progenitor cells has been found to be HIF mediated, with higher numbers found in circulation in patients with PAH than in healthy volunteers (10, 20). At the same time, this study reports a drop in the percent of $CD34^+CD133^+$ cells in patients with PAH over time, with percent change in $CD34^+CD133^+$ cells negatively associated with percent changes in ventricular FDG-SUV over 1 year. Despite the small numbers, those that maintained a steady number of circulating $CD34^+CD133^+$ cells were more likely to have a decrease in ventricular FDG-SUV, pointing to a possible protective effect. Although erythropoietin expression is also mediated by HIF activation and the levels are high in PAH and relate to the proliferative vasculopathy (10), erythropoietin was not related to RV glucose uptake or failure in the present study. Another group hypothesized that increased FDG-SUV may be due to increased inflammation in the disease; however, they did not detect any correlations between RV FDG-SUV and CRP or inflammatory cytokines (8).

Although HIF expression in the cardiomyocytes of hearts from patients with PAH is consistent with the finding of greater glucose uptake, whether or not HIF has a causal role in the glycolytic shift of the PAH heart awaits mechanistic experiments or quantitative metrics of tissue glucose utilization. Hypoxia classically stabilizes HIF-1α, leading to the induction of HIF-regulated genes, but the patients with PAH included in this study were generally not hypoxic, consistent with the notion that PAH is associated with an inappropriate, normoxic activation of HIF-1α. Nevertheless, transient exercise-induced hypoxia or low mixed venous oxygen may contribute to the activation of HIF in some patients with PAH, which was not directly assessed in this study. In addition to these possibilities, a variety of mechanisms have been identified in prior studies to explain enhanced expression of HIF-1α in PAH. Archer and colleagues described the activation of HIF via loss of reactive oxygen species secondary to mitochondrial abnormalities (28, 29), whereas others have related HIF expression in PAH to dysregulation in NO metabolism (11, 12). Both of these theories center around observed mitochondrial abnormalities and a reduction in the mitochondrial antioxidant superoxide dismutase-2, which

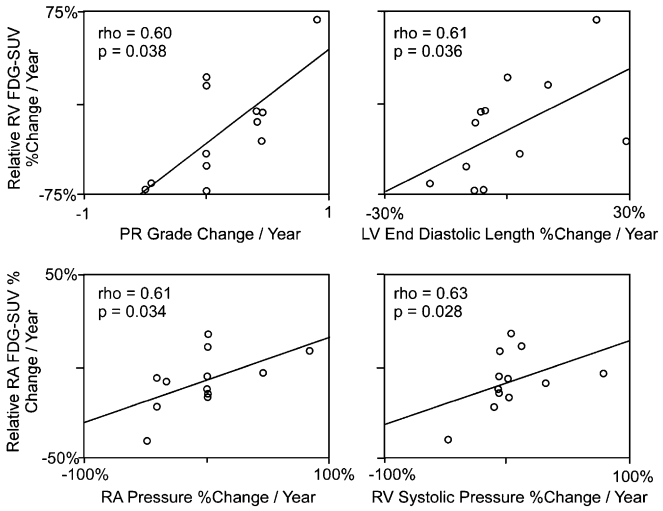

Figure 7. Percent changes in fasting relative 2-deoxy-2-[^{18}F]fluoro-D-glucose standardized uptake value (FDG-SUV) over 1 year correlates with changes in echocardiographic disease severity measures. Each *open circle* represents an independent patient with pulmonary arterial hypertension. LV = left ventricle; PR = pulmonary regurgitation; RA = right atrium; RV = right ventricle.

has recently been discovered to be silenced epigenetically via hypermethylation in the fawn hooded rat model of PAH (30). Additionally, alterations in cellular microRNAs have recently been implicated in PAH (31–33), and a handful of microRNAs have been shown to modify HIF expression in either a hypoxia-dependent (34–36) or hypoxia-independent (37–39) fashion. The pulmonary arterial endothelial cells from lungs of patients with PAH contain decreased mitochondrial numbers (11). Similarly, mitochondrial gene expression decreases with increases in RV pressure, with depletion of mitochondrial DNA in heart failure due to congenital heart diseases that cause chronic hemodynamic overload (40). Murine models shed light on the mechanistic role of HIF-1α in the myocardium. Mice that are heterozygous for the null HIF-1α allele appear identical to wild-type mice but develop significantly less RV hypertrophy and pulmonary arteriolar muscularization in response to chronic hypoxia (41). Overexpression of HIF-1α produces the opposite effect. Mice with genetic deletion of von Hippel Lindau (VHL) protein, which regulates degradation of HIF, have higher levels of HIF-1α than wild-type mice and develop severe heart failure associated with myocyte loss, fibrosis, lipid accumulation, nuclear abnormalities, and loss of mitochondria (42). These abnormalities were reversed by cardiac-specific double deletion of VHL and HIF-1α genes, suggesting these maladaptive changes in the heart are due to chronic elevation of HIF-1α (42). In the murine VHL knockout, cellular changes of the myocardium were consistent with autophagy, providing support for the concept that chronic HIF activation leads to cellular starvation irrespective of availability of nutrients (42). Hence, it is conceivable that a switch to predominantly glycolytic metabolism impairs the heart's ability to use nutrients optimally, further contributing to cardiac pathologic remodeling and failure.

There are limitations to the current study. First, we were unable to directly measure the HIF-1α expression of the hearts of participants undergoing FDG-PET and therefore cannot directly associate HIF-1α expression with fasting FDG uptake. Instead, we used explanted PAH and control hearts to evaluate tissue expression of HIF-1α and measured biomarkers in the participants that are related to HIF activation. Additionally, the sample size is small, such that subgroup analyses for different types of PAH was not possible, and only patients who had already been optimized on PAH therapies were recruited. Furthermore, the number of patients that clinically worsened over the year was small in this cohort, limiting our ability to draw conclusions regarding the utility of FDG-PET in PAH monitoring. Nevertheless, the strong relationship observed with echocardiographic measures of RV structure and function provides promise that FDG-PET may be helpful in patient care. Finally, this study has limitations of possible confounding by treatment or other underlying characteristics of patients. However, a strength of this study is that the majority of our PAH cohort was followed up 1 year later, allowing us to evaluate changes in RV structure, function, and metabolism over time.

The current findings suggest that fasting FDG-PET may provide mechanistic evaluation of RV failure in patients with PAH. Additional longitudinal studies on treatment-naive (newly diagnosed) patients with PAH and longer times of follow-up are required to help determine whether fasting FDG-PET can be clinically helpful in the quantitative assessment of right heart function and in the monitoring of patients with PAH. Future study is therefore planned to investigate the use of FDG-PET in relationship to introduction of new therapy. The current study points toward new therapeutic targets in PAH, and future work is needed to evaluate whether metabolic modulation preserves RV function. ■

Author disclosures are available with the text of this article at www.atsjournals.org.

Acknowledgment: The authors thank Denise Hatala (immunohistochemistry) in the Lerner Research Institute Digital Imaging Core and Moneen Morgan, Sage O'Bryant, and Cathy Shemo in the Flow Cytometry core for technical assistance with instrument operation.

References

1 Firth AL, Mandel J, Yuan J X-J. Idiopathic pulmonary arterial hypertension. *Dis Model Mech* 2010;3:268–273.

2 Humbert M, Sitbon O, Chaouat A, Bertocchi M, Habib G, Gressin V, Yaïci A, Weitzenblum E, Cordier JF, Chabot F, *et al*. Survival in patients with idiopathic, familial, and anorexigen-associated pulmonary arterial hypertension in the modern management era. *Circulation* 2010;122:156–163.

3 Toblli JE, Lombraña A, Duarte P, Di Gennaro F. Intravenous iron reduces NT-pro-brain natriuretic peptide in anemic patients with chronic heart failure and renal insufficiency. *J Am Coll Cardiol* 2007;50:1657–1665.

4 Sztrymf B, Souza R, Bertoletti L, Jaïs X, Sitbon O, Price LC, Simonneau G, Humbert M. Prognostic factors of acute heart failure in patients

with pulmonary arterial hypertension. *Eur Respir J* 2010. 35: 1286–1293.
5 WXisneski JA, Gertz EW, Neese RA, Mayr M. Myocardial metabolism of free fatty acids: studies with 14C-labeled substrates in humans. *J Clin Invest* 1987;79:359–366.
6 Can MM, Kaymaz C, Tanboga IH, Tokgoz HC, Canpolat N, Turkyilmaz E, Sonmez K, Ozdemir N. Increased right ventricular glucose metabolism in patients with pulmonary arterial hypertension. *Clin Nucl Med* 2011; 36:743–748.
7 Oikawa M, Kagaya Y, Otani H, Sakuma M, Demachi J, Suzuki J, Takahashi T, Nawata J, Ido T, Watanabe J, Shirato K. Increased [18F] fluorodeoxyglucose accumulation in right ventricular free wall in patients with pulmonary hypertension and the effect of epoprostenol. *J Am Coll Cardiol* 2005;45:1849–1855.
8 Hagan G, Southwood M, Treacy C, Ross RM, Soon E, Coulson J, Sheares K, Screaton N, Pepke-Zaba J, Morrell NW, Rudd JH. (18) FDG PET imaging can quantify increased cellular metabolism in pulmonary arterial hypertension: a proof-of-principle study. *Pulm Circ* 2011;1:448–455.
9 Semenza GL. Oxygen sensing, homeostasis, and disease. *N Engl J Med* 2011;365:537–547.
10 Farha S, Asosingh K, Xu W, Sharp J, George D, Comhair S, Park M, Tang WH, Loyd JE, Theil K, *et al*. Hypoxia-inducible factors in human pulmonary arterial hypertension: a link to the intrinsic myeloid abnormalities. *Blood* 2011;117:3485–3493.
11 Xu W, Koeck T, Lara AR, Neumann D, DiFilippo FP, Koo M, Janocha AJ, Masri FA, Arroliga AC, Jennings C, *et al*. Alterations of cellular bioenergetics in pulmonary artery endothelial cells. *Proc Natl Acad Sci USA* 2007;104:1342–1347.
12 Fijalkowska I, Xu W, Comhair SA, Janocha AJ, Mavrakis LA, Krishnamachary B, Zhen L, Mao T, Richter A, Erzurum SC, Tuder RM, *et al*. Hypoxia inducible-factor1alpha regulates the metabolic shift of pulmonary hypertensive endothelial cells. *Am J Pathol* 2010; 176:1130–1138.
13 Lundgrin EL, Park MM, Sharp J, Tang WHW, Thomas JD, Asosingh K, Comhair SA, DiFilippo FP, Neumann DR, Graham BB, *et al*. Glycolytic metabolism in hearts of pulmonary arterial hypertension patients [abstract]. *Am J Respir Crit Care Med* 2012;185:A3450.
14 Rudski LG, Lai WW, Afilalo J, Hua L, Handschumacher MD, Chandrasekaran K, Solomon SD, Louie EK, Schiller NB. Guidelines for the echocardiographic assessment of the right heart in adults: a report from the American Society of Echocardiography endorsed by the European Association of Echocardiography, a registered branch of the European Society of Cardiology, and the Canadian Society of Echocardiography. *J Am Soc Echocardiogr* 2010;23: 685–713; quiz 786–788.
15 Ryan T, Petrovic O, Dillon JC, Feigenbaum H, Conley MJ, Armstrong WF. An echocardiographic index for separation of right ventricular volume and pressure overload. *J Am Coll Cardiol* 1985;5:918–927.
16 Louie EK, Rich S, Levitsky S, Brundage BH. Doppler echocardiographic demonstration of the differential effects of right ventricular pressure and volume overload on left ventricular geometry and filling. *J Am Coll Cardiol* 1992;19:84–90.
17 McGoon M, Gutterman D, Steen V, Barst R, McCrory DC, Fortin TA, Loyd JE; American College of Chest Physicians. Screening, early detection, and diagnosis of pulmonary arterial hypertension: ACCP evidence-based clinical practice guidelines. *Chest* 2004;126: 14S–34S.
18 American Thoracic Society. ATS statement: guidelines for the six-minute walk test. *Am J Respir Crit Care Med* 2002;166:111–117.
19 van Wolferen SA, Marcus JT, Boonstra A, Marques KM, Bronzwaer JG, Spreeuwenberg MD, Postmus PE, Vonk-Noordegraaf A. Prognostic value of right ventricular mass, volume, and function in idiopathic pulmonary arterial hypertension. *Eur Heart J* 2007;28:1250–1257.
20 Asosingh K, Aldred MA, Vasanji A, Drazba J, Sharp J, Farver C, Comhair SA, Xu W, Licina L, Huang L, *et al*. Circulating angiogenic precursors in idiopathic pulmonary arterial hypertension. *Am J Pathol* 2008;172:615–627.
21 Mielniczuk LM, Birnie D, Ziadi MC, deKemp RA, DaSilva JN, Burwash I, Tang AT, Davies RA, Haddad H, Guo A, *et al*. Relation between right ventricular function and increased right ventricular [18F] fluorodeoxyglucose accumulation in patients with heart failure. *Circ Cardiovasc Imaging* 2011;4:59–66.
22 Kluge R, Barthel H, Pankau H, Seese A, Schauer J, Wirtz H, Seyfarth HJ, Steinbach J, Sabri O, Winkler J. Different mechanisms for changes in glucose uptake of the right and left ventricular myocardium in pulmonary hypertension. *J Nucl Med* 2005;46:25–31.
23 Wong YY, Ruiter G, Lubberink M, Raijmakers PG, Knaapen P, Marcus JT, Boonstra A, Lammertsma AA, Westerhof N, van der Laarse WJ, *et al*. Right ventricular failure in idiopathic pulmonary arterial hypertension is associated with inefficient myocardial oxygen utilization. *Circ Heart Fail* 2011;4:700–706.
24 Bokhari S, Raina A, Rosenweig EB, Schulze PC, Bokhari J, Einstein AJ, Barst RJ, Johnson LL. PET imaging may provide a novel biomarker and understanding of right ventricular dysfunction in patients with idiopathic pulmonary arterial hypertension. *Circ Cardiovasc Imaging* 2011;4:641–647.
25 Marsboom G, Wietholt C, Haney CR, Toth PT, Ryan JJ, Morrow E, Thenappan T, Bache-Wiig P, Piao L, Paul J, Chen CT, Archer SL. Lung ^{18}F-fluorodeoxyglucose positron emission tomography for diagnosis and monitoring of pulmonary arterial hypertension. *Am J Respir Crit Care Med* 2012;185:670–679.
26 Bogaard HJ, Natarajan R, Henderson SC, Long CS, Kraskauskas D, Smithson L, Ockaili R, McCord JM, Voelkel NF. Chronic pulmonary artery pressure elevation is insufficient to explain right heart failure. *Circulation* 2009;120:1951–1960.
27 Batal O, Khatib OF, Dweik RA, Hammel JP, McCarthy K, Minai OA. Comparison of baseline predictors of prognosis in pulmonary arterial hypertension in patients surviving $\leqslant$2 years and those surviving $\geqslant$5 years after baseline right-sided cardiac catheterization. *Am J Cardiol* 2012;109:1514–1520.
28 Archer SL, Gomberg-Maitland M, Maitland ML, Rich S, Garcia JG, Weir EK. Mitochondrial metabolism, redox signaling, and fusion: a mitochondria-ROS-HIF-1alpha-Kv1.5 O2-sensing pathway at the intersection of pulmonary hypertension and cancer. *Am J Physiol Heart Circ Physiol* 2008;294:H570–H578.
29 Bonnet S, Michelakis ED, Porter CJ, Andrade-Navarro MA, Thébaud B, Bonnet S, Haromy A, Harry G, Moudgil R, McMurtry MS, *et al*. An abnormal mitochondrial-hypoxia inducible factor-1alpha-Kv channel pathway disrupts oxygen sensing and triggers pulmonary arterial hypertension in fawn hooded rats: similarities to human pulmonary arterial hypertension. *Circulation* 2006;113:2630–2641.
30 Archer SL, Marsboom G, Kim GH, Zhang HJ, Toth PT, Svensson EC, Dyck JR, Gomberg-Maitland M, Thébaud B, Husain AN, *et al*. Epigenetic attenuation of mitochondrial superoxide dismutase 2 in pulmonary arterial hypertension: a basis for excessive cell proliferation and a new therapeutic target. *Circulation* 2010;121:2661–2671.
31 Courboulin A, Paulin R, Giguère NJ, Saksouk N, Perreault T, Meloche J, Paquet ER, Biardel S, Provencher S, Côté J, *et al*. Role for miR-204 in human pulmonary arterial hypertension. *J Exp Med* 2011;208: 535–548.
32 Caruso P, MacLean MR, Khanin R, McClure J, Soon E, Southgate M, MacDonald RA, Greig JA, Robertson KE, Masson R, *et al*. Dynamic changes in lung microRNA profiles during the development of pulmonary hypertension due to chronic hypoxia and monocrotaline. *Arterioscler Thromb Vasc Biol* 2010;30:716–723.
33 Drake KM, Zygmunt D, Mavrakis L, Harbor P, Wang L, Comhair SA, Erzurum SC, Aldred MA. Altered microRNA processing in heritable pulmonary arterial hypertension: an important role for Smad-8. *Am J Respir Crit Care Med* 2011;184:1400–1408.
34 Rane S, He M, Sayed D, Vashistha H, Malhotra A, Sadoshima J, Vatner DE, Vatner SF, Abdellatif M. Downregulation of miR-199a derepresses hypoxia-inducible factor-1alpha and Sirtuin 1 and recapitulates hypoxia preconditioning in cardiac myocytes. *Circ Res* 2009;104:879–886.
35 Ghosh G, Subramanian IV, Adhikari N, Zhang X, Joshi HP, Basi D, Chandrashekhar YS, Hall JL, Roy S, Zeng Y, *et al*. Hypoxia-induced microRNA-424 expression in human endothelial cells regulates HIF-α isoforms and promotes angiogenesis. *J Clin Invest* 2010;120: 4141–4154.
36 Cascio S, D'Andrea A, Ferla R, Surmacz E, Gulotta E, Amodeo V, Bazan V, Gebbia N, Russo A. miR-20b modulates VEGF expression by

targeting HIF-1 alpha and STAT3 in MCF-7 breast cancer cells. *J Cell Physiol* 2010;224:242–249.
37 Taguchi A, Yanagisawa K, Tanaka M, Cao K, Matsuyama Y, Goto H, Takahashi T. Identification of hypoxia-inducible factor-1 alpha as a novel target for miR-17–92 microRNA cluster. *Cancer Res* 2008;68: 5540–5545.
38 Liu C-J, Tsai MM, Hung PS, Kao SY, Liu TY, Wu KJ, Chiou SH, Lin SC, Chang KW. miR-31 ablates expression of the HIF regulatory factor FIH to activate the HIF pathway in head and neck carcinoma. *Cancer Res* 2010;70:1635–1644.
39 Cha S-T, Chen PS, Johansson G, Chu CY, Wang MY, Jeng YM, Yu SL, Chen JS, Chang KJ, Jee SH, *et al*. MicroRNA-519c suppresses hypoxia-inducible factor-1 alpha expression and tumor angiogenesis. *Cancer Res* 2010;70:2675–2685.
40 Karamanlidis G, Bautista-Hernandez V, Fynn-Thompson F, Del Nido P, Tian R. Impaired mitochondrial biogenesis precedes heart failure in right ventricular hypertrophy in congenital heart disease. *Circ Heart Fail* 2011;4:707–713.
41 Yu AY, Shimoda LA, Iyer NV, Huso DL, Sun X, McWilliams R, Beaty T, Sham JS, Wiener CM, Sylvester JT, *et al*. Impaired physiological responses to chronic hypoxia in mice partially deficient for hypoxia-inducible factor 1alpha. *J Clin Invest* 1999; 103:691–696.
42 Lei L, Mason S, Liu D, Huang Y, Marks C, Hickey R, Jovin IS, Pypaert M, Johnson RS, Giordano FJ. Hypoxia-inducible factor-dependent degeneration, failure, and malignant transformation of the heart in the absence of the von Hippel-Lindau protein. *Mol Cell Biol* 2008;28: 3790–3803.